

The determination of percentage dissociation of zircon (ZrSiO_4) to plasma-dissociated zircon (ZrO_2SiO_2) by Raman spectroscopy

L. D. Kock,* M. D. S. Lekgoathi, E. Snyders, J. B. Wagener, J. T. Nel and J. L. Havenga

Raman spectroscopy and multivariate calibration techniques are used to determine the percentage conversion of zircon (ZrSiO_4) to plasma-dissociated zircon, ZrO_2SiO_2 (PDZ). The integrated area of a consistent ZrO_2 (monoclinic) Raman band at 477 cm^{-1} assigned to the A_g symmetry type from different conversion percentages of the PDZ spectra is used in a multivariate analysis scheme (partial least squares) to develop a predictive model for the subsequent determination of percentage dissociation of zircon to PDZ. In contrast to wet chemical methods, this approach eliminates the use of corrosive acids, e.g. hydrofluoric acid, thus leading to significant reductions in analysis time and material wastage, and it is a quick method that can be used online in a PDZ production facility. These results show best correlation with determination coefficient (R^2) values in the range between 99.45 and 99.99% for zircon percentage dissociation in cross-validation tests. This illustrates not only the versatility of the Raman technique in industrial applications but also the importance of noninvasive testing in the study of zircon and related materials. Copyright © 2011 John Wiley & Sons, Ltd.

Keywords: FT-Raman; plasma-dissociated zircon; percentage dissociation; zircon

Introduction

Zircon mineral is the ground-state polymorph of the structure ZrSiO_4 , which may be converted at high temperature (1200 K) and pressure (12 GPa) to scheelite-type Reidite crystals.^[1,2] This type of conversion is reversible at 1500 K.^[3] The zircon mineral structure contains interstices appropriate for hosting rare earth elements and indeed it is often found containing uranium and thorium in the earth's crust. It is for this reason that zircon is often considered as a natural host material for the storage of radioactive waste material.^[1,4] Zirconium silicate (ZrSiO_4) is also considered as a promising alternative to silicon oxide as the gate dielectric material in metal-oxide semiconductor devices because of its high permittivity.^[1] By using plasma conversion technology, the mineral zircon can also be converted to plasma-dissociated zircon consisting of submicron, monoclinic ZrO_2 particles cemented together by amorphous silica (SiO_2).^[5] The space group for zircon (ZrSiO_4) is $I4_1/amd$ ($Z=4$) (D_{4h}^{19})^[6] and from group theory considerations, 12 Raman active modes are predicted ($2A_{1g} + 4B_{1g} + B_{2g} + 5E_g$). On the other hand, zirconium oxide (ZrO_2) exists in three polymorphic forms, namely: (1) monoclinic, which has space group $P2_1/b$ (C_{2h}^5) and $Z=4$ has 18 Raman active modes $9A_g + 9B_g$; (2) the tetragonal phase (ZrO_2), space group $P4_2/mnc$ (D_{4h}^{15}) and $Z=2$ has six Raman active modes, $A_{1g} + 2B_{1g} + 3E_g$; and (3) the cubic phase, space group $Fm3m$ (O_h^5), $Z=4$ with only one Raman active mode.^[7] Given these differences, one may differentiate one phase from the others on the basis of their Raman spectrum in interpreting the plasma-dissociated zircon (PDZ) spectra.

The use of PDZ in the production of zirconium-based pigments has previously been described^[8] and the effect of milling and percentage dissociation of PDZ on the colour of Pr-yellow and

V-blue doped-zircon pigments has also been investigated.^[9] However, the percentage dissociation determination of PDZ in zircon by Raman spectroscopy and multivariate techniques has not been reported. Because zircon's chemical reaction susceptibility is increased by dissociation to PDZ,^[5] the question of the extent of this dissociation becomes important in determining limiting reaction conditions in the manufacturing of PDZ and the subsequent chemical processing thereof.

The manufacturing of PDZ was described by Wilks *et al.*^[10], Fridman^[11] and Toumanov.^[12] There are several parameters that influence the manufacturing of PDZ. These are the applied plasma power, the particle size of the zircon, the geometry of the plasmatron and plasma reactor, the residence time of the particle in the reaction zone and the quenching rate of the PDZ particle. No significant changes in the chemical composition of the zircon and the PDZ could be found in this study.^[13] Inductively coupled plasma spectrometry analysis of zircon and PDZ are presented in Table 1. The different commercial grades of zircon are generally classified as prime grade (purity > 99.3%), standard grade (purity 98–99%) and refractory grade (purity ~95%). In this study, prime-grade zircon from Namakwa Sands was used. The d_{50} particle size of this zircon was 125 μm , as determined by the Sedigraph technique. When zircon is converted into PDZ, spheridization takes place with the PDZ particle almost perfectly spherical with a d_{50} value of 105 μm . Scanning electron

* Correspondence to: L. D. Kock, Department of Applied Chemistry, The South African Nuclear Energy Corporation Limited (Necsa), P.O. Box 582, Pretoria 0001, South Africa. E-mail: david.kock@necsa.co.za

Department of Applied Chemistry, The South African Nuclear Energy Corporation Limited (Necsa), P.O. Box 582, Pretoria, 0001, South Africa

Table 1. Inductively coupled plasma spectrometry analysis results of the chemical composition of zircon and PDZ

Compound/element	Units ^a	Zircon	PDZ
ZrO ₂ (HfO ₂) ^b	%	66.7	66.6
SiO ₂	%	32.6	32.7
TiO ₂	%	0.12	0.12
Fe ₂ O ₃	%	0.06	0.06
Al ₂ O ₃	%	0.07	0.09
MgO	%	0.01	0.02
CaO	%	0.05	0.04
P ₂ O ₅	%	0.10	0.09
U + Th	%	<500	<500

^aThe accuracy of the chemical analysis for the above mentioned oxides is $\pm 0.1\%$ and for U + Th it is $\pm 50 \text{ mg}\cdot\text{kg}^{-1}$.

^bZircon always contain hafnium oxide (1–3%) and their concentrations are usually reported together.

microscopy investigations (Fig. 1) of a cross-cut section of a PDZ particle, showed that the monoclinic zirconia particles that formed (white dots) are about $0.2 \mu\text{m}$ in diameter and these are uniformly distributed in the amorphous silica matrix and the big ($105 \mu\text{m}$) PDZ particle.

Because the selection rules in Raman spectroscopy depend on molecular structure,^[14] the Raman technique is ideally suited to study the transition from ZrSiO_4 to $\text{ZrO}_2\cdot\text{SiO}_2$ (PDZ). Raman spectroscopy has previously been used successfully in the study of pigment sample mixtures without signal interference^[15–17] and together with multivariate techniques, Raman provided yet another useful method for determining component concentrations in multicomponent drug products.^[18] This technique has also previously been used to study atmospheric residues of petroleum products,^[19] the weight percent of oxygen in gasoline^[20] and quantitative analysis of paracetamol polymorph mixtures.^[21]

Several improvements in the methods of acquisition of Raman spectra, including the use of excitation radiation in the near-infrared region to minimize fluorescence effects and the use of charge-coupled device detectors with Fourier transform

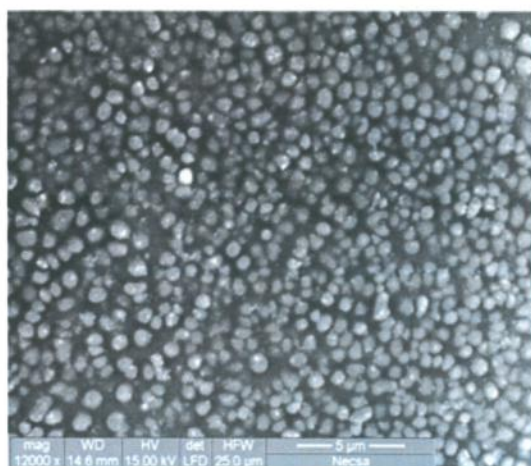


Figure 1. The scanning electron microscopy image of a cross-section of a PDZ particle is presented showing the monoclinic zirconia particle size of $0.2 \mu\text{m}$ in diameter.

(FT)–Raman instruments greatly improved the reproducibility of the Raman spectra, leading to increased use of multivariate analysis techniques with Raman spectroscopy.^[22,23]

In this paper, we present the results of the determination of percentage dissociation of the mineral zircon by FT–Raman spectroscopy and multivariate calibration techniques. The tremendous advantages of this approach are due to minimal sample handling requirements, ease of instrument use and low turn-around time.^[24] The results are compared with those obtained from more tedious and lengthy wet-chemical methods.^[25]

Experimental Procedure and Materials

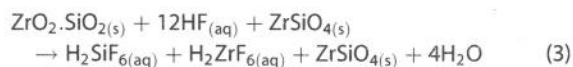
The production of PDZ using plasma conversion technology was carried out at the South African Nuclear Energy Corporation (Necsa) and has been adequately described elsewhere.^[9–12] The PDZ synthesis method is essentially comprised of allowing zircon particles to free fall through a plasma reaction chamber at temperatures exceeding 1800°C , followed by a rapid product-cooling rate control for optimum product formation^[1–3] In general, the percentage dissociation of the zircon is dependent on various interdependent parameters, for example, the applied plasma power, the particle size of the zircon, the feed rate of the zircon, the quenching rate of the product, etc.

Metamictization (radiation damage) does occur in zircon, but usually this is only observable in zircons that received high dosages of radiation leading to the destruction of its lattice crystal structure. This is a result of the α -decay from uranium and thorium that is usually encapsulated in zircon and is also a function of the intensity and duration of the radiation.^[26] In this study, zircon containing U + Th $< 500 \text{ mg kg}^{-1}$ was used and no significant metamictization could be observed.

The synthesized samples were placed in the macrochamber of the Bruker Vertex 70 FT-Raman machine (Ram II module mounted onto a vertex 70 FT-IR) for Raman acquisition. A 1064 nm wavelength excitation radiation with a 50 mW power setting and a 4 cm^{-1} spectral resolution on the instrument was used. The integration times were set at typically 30 s with one accumulation per spectral window, and the entire analysis could be completed within about 20 min . Zircon (prime grade) was obtained from Namakwa Sands (Pty) Ltd and the 100% converted PDZ was supplied by Zeetech LLC, USA. The samples with various percentages of PDZ composition (82, 90, 94, 95 and 96%) were manufactured by Necsa under various plasma conditions in a $3 \times 150 \text{ kW DC}$ plasma plant.

Results and Discussion

Taking advantage of the insolubility of ZrSiO_4 in hydrofluoric acid (HF) versus the complete solubility of PDZ in HF, a wet-chemical method for determining the percentage of PDZ in the zircon/PDZ mixture involves the dissolution of zircon/PDZ mixture in 40% HF.^[25] The wet chemical gravimetric determination of the percentage dissociation of zircon to PDZ is based on the difference in reactivity of zircon and PDZ toward hydrofluoric acid. At room temperature, zircon (ZrSiO_4) is chemically inert towards HF (Reaction (1)), while PDZ ($\text{ZrO}_2\cdot\text{SiO}_2$) reacts with HF exothermically and all plasma-dissociated zircon dissolve according Reaction (2). Combining reactions (1) and (2) below, we may represent this process as in Reaction (3).



This allows for the calculation of the required percentage of dissociated zircon (PDZ) in the zircon/PDZ mixture within an accuracy of 0.5%. This lengthy gravimetric method, including the dissolution steps, neutralization, filtration, washing and drying, takes at least 4 h to produce a result.

Figure 2 shows typical Raman spectra of (a) $ZrSiO_4$ (tetragonal), (b) PDZ and (c) ZrO_2 (baddeleyite) with monoclinic structure. A set of spectra depicting various percent PDZ concentrations between 100% $ZrSiO_4$ (Fig. 2(a)) and 100% PDZ (Fig. 2(b)) have been omitted. $ZrSiO_4$ and ZrO_2 have received considerable attention in the literature.^[27–31] It must also be noted that the differentiation between monoclinic and amorphous zirconia is very difficult because of the Raman band overlap.^[32] The region between 500 and 700 cm^{-1} has been identified to show Raman bands that are associated with amorphous zirconia.^[32] As a result, one cannot completely rule out the presence of amorphous zirconia, because the monoclinic phase does also show Raman bands in this region. With due consideration to the foregoing discussion, Table 2 depicts a summary of literature Raman band assignments and provides confirmation that the ZrO_2 in our PDZ is largely of monoclinic structure in Reaction (4);



Using a multivariate calibration scheme as coded in the QUANT module of the OPUSTM software program^[33] using partial least square (PLS), a predictive model of determining % PDZ in zircon samples was developed. Applications of multivariate methods with Raman spectroscopy for quantitative calibrations have been discussed.^[22,23,34–37] The basic aim of the method is to determine a property Y from an experimentally observable X (such as concentration) that is correlated by a calibration function b ($Y = X \cdot b$). The row vectors of the matrix X are

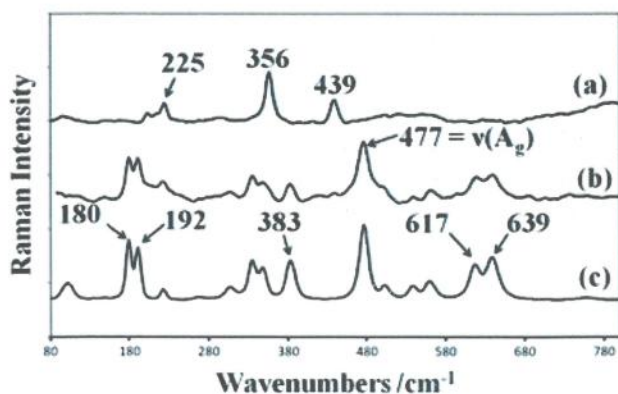


Figure 2. Raman spectra of (a) the mineral zircon ($ZrSiO_4$); (b) plasma-dissociated zircon (ZrO_2SiO_2 or PDZ) with the 477 cm^{-1} ($\nu(A_g)$) Raman band of ZrO_2 indicated with an arrow; and (c) ZrO_2 (monoclinic (space group: $P2_1/b$ (C_2h))).

formed from the calibration spectra, while the vector Y consists of single component values determined from a reference method. The solution for b may then be written as

$$b = (X^T \cdot X)^{-1} \cdot (X^T \cdot Y) \quad (5)$$

In PLS, the solution of Eqn 5 is achieved by the calculation of a restricted inverse instead of a complete inverse (because of the difficulty in inverting $X^T \cdot X$). A starting vector (v_1) is chosen such that;

$$v_1 = \frac{X^T \cdot Y}{X^T \cdot Y} \quad (6)$$

A PLS regression analysis is then continued until the component values Y are reproduced in a consistent way. In the QUANT module of the OPUS program,^[33] the optimum PLS vector is

Table 2. A comparison of the Raman bands (cm^{-1}) of different phases of ZrO_2 compared with those of zircon and PDZ

Zircon $ZrSiO_4$	PDZ ZrO_2SiO_2	Monoclinic ZrO_2	Tetragonal ZrO_2	Cubic ZrO_2
	Raman/ cm^{-1}	Raman/ cm^{-1} [27,28]	Raman/ cm^{-1} [27,29]	Raman/ cm^{-1} [27,30,31]
		37		
		103		
	118 w			
	121 w		122 m	
	178 m	180	180 w	
	190 m	192	192 w	
200 w				
213 w				
223 w	223 m	224		245 b w ?
	309 vw	308		
			278 s	
			319 m	
		336		
355 s		348		
		383	380 w	
391 vw				
439 s	477 m	477	460 m	
			480 m sh	
	504 w	503		
517 vw b				
	536 b w	537		
	562 vw	561		(534 – 640 b) ?
	600 vvw		600 vw	590 b w
	618 m	617	618 m sh	
	640 m	639	641 s	
662 vw b				
	744 vvw	735		
974 m				
1007 s				
1054 vw				
1090 vw				
1113 vw				
1159 vw				

Table 3. The quality of validation results for the four series shown in Figs 2(a)–(d)

No.	Frequency range (cm ⁻¹)	Optimum rank	Coefficient determination, R ² (%)	Residual prediction deviation	RMSEE
1	455–495	3	99.45	13.5	3.74
2	455–495	3	96.45	5.22	9.66
3	455–495	4	99.99	135	0.459
4	455–495	4	99.86	26.8	2.3

determined only when the number of calibration spectra per component is deemed sufficient.^[33] The difference between the true concentration (C_k , with the average denoted by \bar{C}_k) and fitted value (C_p) is then used to determine the root mean square error of estimation (RMSEE) in Eqn 8, where m is the number of standards used, r is the rank and R in Eqn 9 is the coefficient of determination. (See also Table 3).

$$SSE = \sum_{i=0}^M (C_{p_i} - \bar{C}_k)^2 \quad (7)$$

$$RMSEE = \sqrt{\frac{1}{m-r-1} SSE} \quad (8)$$

$$R^2 = \left[1 - \frac{SSE}{\sum_{i=0}^M (C_{p_i} - \bar{C}_k)^2} \right] \times 100 \quad (9)$$

The coefficient of determination (R^2) approaches 100% as the fitted concentration values approach the true values as expected.

The $\nu(A_g)$ Raman band at 477 cm⁻¹ was used in the calibrations. Figures 3(a)–(d) show calibration series plots that were generated for various percentages of PDZ. The plots show the 'Fit versus True' graph for four series of percentage PDZ using the various PDZ concentrations (0, 82, 90, 94, 95, 96 and 100%). Figure 4 shows the change in intensity of the Raman band ($\nu(A_g)=477\text{ cm}^{-1}$) corresponding to the various percentages (0, 82, 90, 94, 95, 96 and 100%) of PDZ in the samples. Outliers do occur from time to time.^[38] Concentration values whose deviation from the true concentration value is statistically significant are detected as possible outliers. Knowledge of these samples is important to help determine whether it is appropriate to exclude these from the model.^[38–40] One such series showed an outlier point (Fig. 3(a) indicated with an arrow) and R^2 value of 99.45% without this point was deemed satisfactory. Table 3 shows a summary of the calibration series also shown in Fig. 3. Series B showed a lower R^2 (96.33%) value and although it was acceptable it was deemed not entirely satisfactory. This series was plotted with a higher residuum threshold and included in the study. The coefficient of determination (R^2) values and residual prediction deviation are presented together with the corresponding optimum rank. The rank in the QUANT program defines the number of PLS vectors that are used and the indicated optimum rank (Table 3) confirms the sufficiency of the number of calibration spectra.

This technique was then applied in the rapid determinations of percent PDZ in zircon and may readily be used in a PDZ manufacturing environment. The immediate effect is

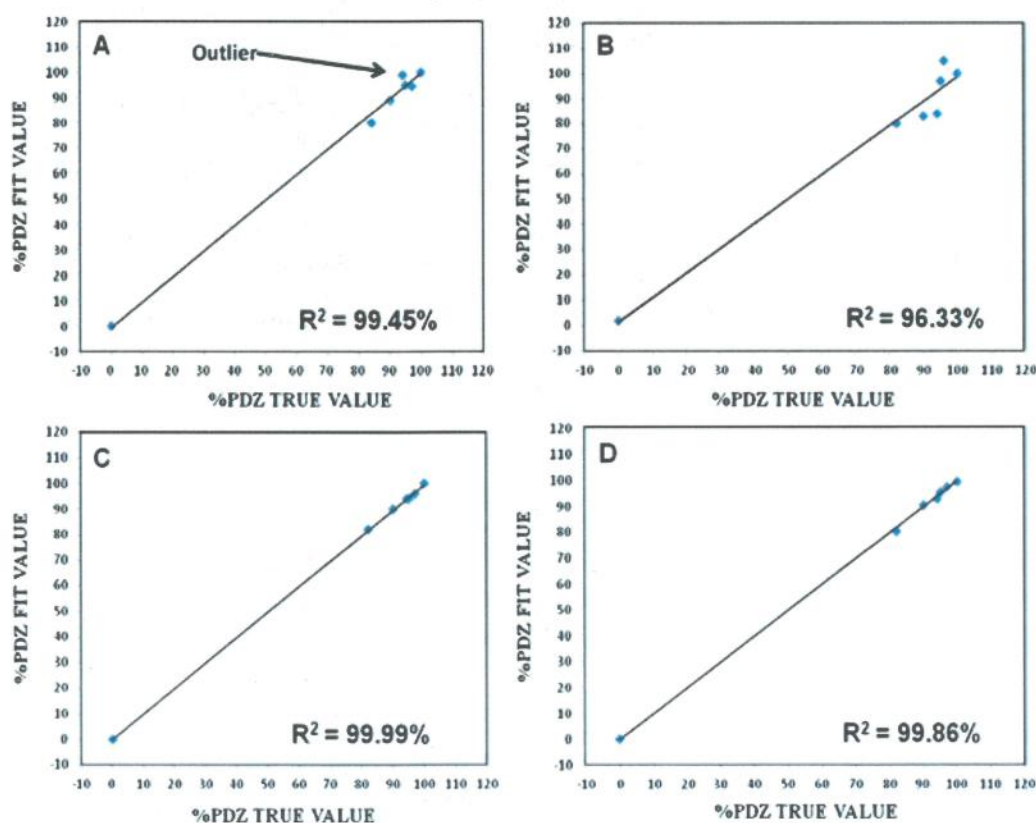


Figure 3. (a)–(d) The four calibration series for various percentages (82, 90, 94, 95, 96 and 100%) of plasma-dissociated zircon, extrapolated to 0%. The area between 455 and 495 cm⁻¹ centred at 477 cm⁻¹ (Fig. 2) was used for the calibration to produce the %PDZ Fit versus %PDZ True values as plotted.

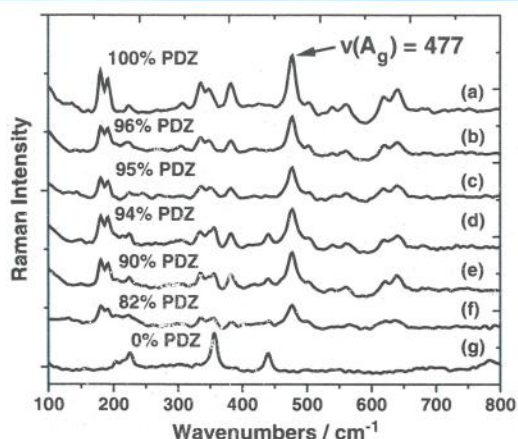


Figure 4. The Raman band at 477 cm^{-1} that was used in the calibrations is shown. The range $455\text{--}495\text{ cm}^{-1}$, was chosen for the preliminary calibrations in Figs 2(a)–(d). The centre of the chosen Raman band is at 477 cm^{-1} ($\nu(A_g)$) and the resulting R^2 value(s) of 99.86% or above that are obtained in the linear fit is acceptable.

the elimination of lengthy processes of determining the percentage dissociation involving wet-chemical methods, resulting in marked reduction in chemical waste and the need for handling corrosive acids such as HF. While it can take up to 4 h using wet chemical techniques, this method can reduce that time to just a few minutes.

Conclusion

A quick and reliable method, using FT-Raman and multivariate analysis, was used to determine the percentage dissociation of the mineral zircon to plasma-dissociated zircon. On the basis of group theory, the predominant ZrO_2 phase produced in the plasma process is shown by Raman spectroscopy to be the monoclinic phase $P2_1/b$ (C_{2h}^5), with only small amounts of the tetragonal $P4_2/mnc$ (D_{4h}^{15}) and the cubic $Fm\bar{3}m$ (O_h^5) phases. Results indicate that despite the multiphase nature of a component of the product (ZrO_2 (monoclinic, tetragonal and cubic)), a Raman band that is associated with the monoclinic phase of ZrO_2 ($\nu(A_g)=477\text{ cm}^{-1}$) proved to be very effective in percent composition determinations and yielded reliably consistent results that may be useful for routine industrial applications. This method eliminates the need to use lengthy wet-chemical methods where highly corrosive acids are routinely used, thus contributing to immediate reductions in chemical waste.

Acknowledgements

This work was supported by the South African Nuclear Energy Corporation Ltd. and the New Metals Development Network of the Advanced Metals Initiative (AMI), funded by the Department of Science and Technology of South Africa.

References

- [1] M. B. Smimov, S. V. Sukhomlinov, S. K. Smimov, *Phys. Rev.* **2010**, *B82*, 0943071.
- [2] A. F. Reid, A. E. Ringwood, *Earth Planet. Sci. Lett.* **1969**, *6*, 205.
- [3] A. Gucsik, M. Zhang, C. Koeberl, E. K. H. Salije, S. A. T. Redfern, J. M. Pruneda, *Mineral. Mag.* **2004**, *68*, 801.
- [4] M. Zhang, E. K. H. Salije, R. C. Ewing, P. Daniel, T. Geisler, *Phys. Chem. Minerals.* **2004**, *31*, 405.
- [5] E. Snyders, Thesis: The upgrading of zircon to superior opacifier. Tswane University of Technology, D.Tech, **2007**.
- [6] S. A. Miller, H. H. Casper, H. E. Rast, *Phys. Rev.* **1968**, *168*, 964.
- [7] D. Gazzoli, G. Mattei, M. Valigi, *J. Raman Spectrosc.* **2007**, *38*, 824.
- [8] H. A. Morriss, J. P. H. Williamson. Production of Calcined Ceramic Pigments. US Patent 4,047,970 **1977**.
- [9] E. Snyders, J. H. Potgieter, J. T. Nel, *J. Eur. Ceram. Soc.* **2006**, *26*, 1599.
- [10] P. H. Wilks, P. Ravinder, C. L. Grant, *Chem. Eng.(Progr.)* **1972**, *68*, 82.
- [11] A. Fridman, *Plasma Chemistry*, Cambridge University Press, London, **2008**, pp. 477–479.
- [12] I. N. Toumanov, *Plasma and High Frequency Processes for Obtaining and Processing Materials in the Nuclear Fuel Cycle*, Nova Science Publishers, Inc., New York, **2003**, pp 96–104.
- [13] E. Snyders, J. H. Potgieter, J. T. Nel, *J. S. Afr. Mining. Metall.*, **2005**, *105* (7), 459.
- [14] I. E. Wachs in *Handbook of Raman Spectroscopy: From the research Laboratory to the process line*, (Eds, I. R. Lewis, H. G. M. Edwards), Marcel Dekker, Inc., New York, NY, **2001**.
- [15] I. M. Bell, R. J. H. Clark, P. J. Gibbs, *Spectrochim. Acta.* **1997**, *53*, 2159.
- [16] H. G. M. Edwards, C. Brooke, J. K. F. Tait, *J. Raman Spectrosc.* **1997**, *28*, 95.
- [17] H. G. M. Edwards, *Microsc. Anal.* **1997**, *59*, 5.
- [18] T. Ueno, K. Urakami, A. Higashi, M. Umamoto, M. Godo, K. Kitamura, *Yakugaku Zasshi* **2005**, *125*, 807.
- [19] H. Chung, M. S. Ku, *Appl. Spectrosc.* **2000**, *54* 239.
- [20] J. P. Cooper, K. L. Wise, W. T. Welch, R. R. Blesoe, M. R. Summer, *Applied Spectrosc.* **1996**, *50*, 917.
- [21] K. Kachrimanis, D. E. Braun, U. J. Griesser, *J. Pharm. Biomed. Anal.* **2007**, *43*, 407.
- [22] M. Shimoyama, H. Maeda, K. Matsukawa, H. Inoue, T. Ninomiya, Y. Ozaki, *Vibrat. Spectrosc.* **1997**, *14*, 253.
- [23] K. P. J. Williams, R. E. Aries, D. J. Cutler, D. P. Lidiard, *Anal. Chem.* **1990**, *62*, 2553.
- [24] J. M. Andrade, S. Garriques, M. De la Guardia, M. Gomez-Carracedo, D. Prada, *Anal. Chim. Acta* **2003**, *482*, 115.
- [25] J. T. Nel, Process for reacting a zirconia based material, US Patent: 5,958,355. **1997**.
- [26] L. Nasdala, G. Imer, D. Wolf, *Eur. J. Min.* **1995**, *7*, 471.
- [27] G. Pretorius Ph.D dissertation: Applied solid state chemistry of zircon ($ZrSiO_4$) and zirconia (ZrO_2), University of Pretoria, **1995**.
- [28] V. G. Keramidis, W. B. White, *J. Am. Ceram. Soc.* **1974**, *57*, 22.
- [29] P. Bouvier, E. Djurado, C. Ritter, A. J. Dianoux, G. Lucazeau, *Int. J. Inorg. Mater.* **2001**, *3*, 647.
- [30] Y. Sobol, K. Voronko, *J. Phys. Chem. Solids.* **2004**, *65*, 1103.
- [31] M. N. Tahir, M. N. L. Gorgishvili, J. Li, T. Gorelik, U. Kolb, L. Nasdala, D. W. Tremel, *Solid State Sci.* **2007**, *9*, 1105.
- [32] S. Karlin, P. Colomban, *J. Am. Ceram. Soc.* **1999**, *82*, 735.
- [33] OPUS™ Software **2007**, Bruker Optik GmbH, Rudolf-Plank-Straße 27, D-76275 Ettlingen.
- [34] M. B. Seasholdz, A. Archibald, A. Lorber, B. R. Kowalski, *Appl. Spectrosc.* **1989**, *43*, 1067.
- [35] J. F. Aust, K. S. Booksh, C. M. Stelman, R. S. Parnas, M. L. Myrick, *Appl. Spectrosc.* **1997**, *51*, 247.
- [36] J. B. Cooper, E. Phillips, J. Flecher, W. T. Welch, US patent, number 5, 684, 580 **1997**.
- [37] M. M. Delgado-Lopez, PhD Thesis, University of New Mexico, **1998**.
- [38] C. E. Miller, *Chemom. Intell. Lab. Syst.* **1995**, *30*, 11.
- [39] C. E. Miller, *J. Chemom.* **2000**, *14*, 513.
- [40] C. E. Miller, *Process Analytical Chemistry*, Blackwell Publishing, Oxford, **2004**.